Composites Part C: Open Access 6 (2021) 100204

Contents lists available at ScienceDirect

Composites Part C: Open Access

journal homepage: www.sciencedirect.com/journal/composites-part-c-open-access

Adhesion-cohesion balance of prepreg tack in thermoset automated fiber placement. Part 1: Adhesion and surface wetting

D. Budelmann [a,*], C. Schmidt [b], D. Meiners [c]

[a] Institute of Polymer Materials and Plastics Engineering, Clausthal University of Technology, Ottenbecker Damm 12, Stade, Germany
[b] Institute of Production Engineering and Machine Tools, Leibniz University Hannover, Ottenbecker Damm 12, Stade, Germany
[c] Institute of Polymer Materials and Plastics Engineering, Clausthal University of Technology, Agricolastr. 6, Clausthal-Zellerfeld, Germany

ARTICLE INFO

Keywords:
Automated fiber placement
Prepreg
Carbon fiber
Epoxy resin
Adhesion
Surface wetting

ABSTRACT

The constitution of prepreg tack in automated fiber placement (AFP) is affected by a sensitive balance between adhesive interfacial bond strength and cohesive strength of the prepreg resin. In an effort to explore the role of interfacial liquid-solid interaction on the tack of commercial aerospace-grade epoxy prepreg, a surface wetting analysis was performed on AFP-related substrates. The standard test liquid combination water/diiodmethane and extracted neat epoxy resin were used for contact angle measurement employing the sessile drop method and the Owens-Wendt-Rabel-Kaelble (OWRK) model. Additional rheological and topographical analyses were carried out to account for viscous resin flow on surfaces of different roughness. The results from the material characterization are discussed against the background of tack measurement by probe tack testing utilizing a rheometer. Significant differences between the investigated surfaces in terms of both the maximum tack level and the onset temperatures of adhesion were found as a function of test parameters relevant for contact formation. General agreement with the experimental tack results was observed employing a topographically extended version of the Dahlquist criterion. For each substrate, a temperature-dependent critical storage modulus could be determined that conforms to the onset temperature of tackiness. Contact angle measurements revealed a correlation between the thermodynamic work of adhesion and maximum tack and, moreover, the tack onset in the adhesive regime when additionally incorporating surface topography. Matching ratios of polar and dispersive surface free energy and surface tension components were found to favor the molecular interaction at the interface between prepreg resin and substrate.

1. Introduction

Automated fiber placement (AFP) and automated tape laying (ATL) are highly productive processes for advanced manufacturing of large composite parts in the aerospace industry. In these processes, thin stripes or sheets of pre-impregnated carbon fibers (prepregs) are laid in a mold by placement heads attached to industrial robots or gantry systems. Subsequent autoclave cure of the laid laminates at 180 °C results in high-performance structural components with excellent strength-to-weight ratios [1]. Despite its high productivity and level of automation, the layup-process is subject to causing different types of defects in the laminate [2]. Although effort has been put towards the development of automated defect detection systems [3,4], substantial research on the causes of defect occurrence can still contribute to more stable manufacturing processes. The formation of defects in AFP is often linked to inadequate levels of material stickiness (tack) and lack of knowledge on how to precisely control it by process adjustment, respectively [5]. This in particular applies to bonding defects such as wrinkling and bridging. Here, prepreg tack counteracts detaching forces that occur during defect formation and is therefore necessary to ensure proper positioning of the prepreg tows.

Prepreg epoxy resins are not primarily tailored towards tack but rather undergo development to meet the thermo-mechanical requirements of cured parts such as high damage tolerance, strength and glass transition temperature T_g. Thus, tack adjustment is not a matter of resin formulation but needs to be performed by b-staging and especially by process adaption during processing. For this purpose, Smith et al. [6] recently presented tack process maps which can help composite manufacturers to account for out time effects of prepreg tack by layup parameter adaption. The most practical approach to control tack

* Corresponding author.
E-mail address: dennis.budelmann@tu-clausthal.de (D. Budelmann).

https://doi.org/10.1016/j.jcomc.2021.100204
Received 7 September 2021; Received in revised form 29 October 2021; Accepted 2 November 2021
Available online 5 November 2021

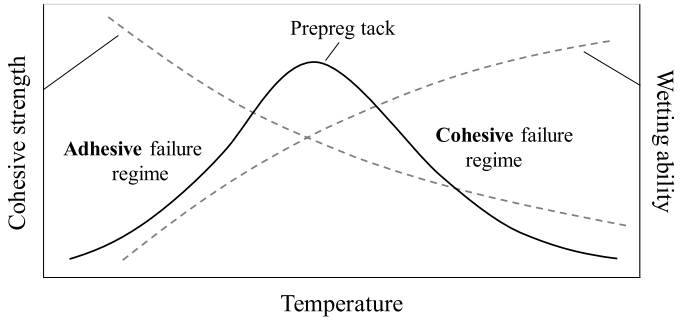

Fig. 1. The temperature-dependent adhesion-cohesion balance of prepreg tack.

throughout the lay-up process is to control the material and mold temperature, e.g., by infrared heaters attached to the AFP machine. Since the very beginning of experimental research on prepreg tack in the 1980s [7], its dependence on the temperature has been a point of focus. Several studies [8–10] have revealed bell-shaped curves independent from the actual test method when plotting experimentally determined prepreg tack as a function of temperature. Evidence was found that the shape of these curves is the result of two major mechanisms which determine the nature of the prepreg's adherence. Similar to the functionality of pressure sensitive adhesives (PSA), maximum stickiness is exhibited when the prepreg matrix on the one hand entirely wets the substrate and on the other hand is able to resist high application loads [11]. The requirements of rapid surface wetting for bond formation and high fracture toughness upon bond separation are partly contradictory as both are highly dependent on the matrix viscosity. An increased flowability constituted by low viscosity will result in enhanced wetting while simultaneously lowering the bearable load. Providing high levels of tack is therefore a matter of sensitive tradeoff which has been described as the adhesion-cohesion balance (Fig. 1) in PSA research [12–14].

While most structural adhesives undergo a phase transition from liquid to solid, e.g., by chemical reaction, solvent evaporation or cooling, PSA and prepregs (during lay-up) remain in a viscoelastic state throughout application and removal. As a consequence, adhesion at the interface cannot be achieved by covalent bonds but has to rely on intermolecular forces (IMF) at the interface which hold the resin/adhesive and the adherend together. IMF with the most common representatives being van der Waals forces and H-bonding, range roughly two magnitudes below covalent bonds in terms of bond energies [15] which makes up for the low separation energies of prepreg tack compared to physically or chemically curing adhesives. A requirement for these forces to be effective is to establish intimate contact between adhesive/resin and the substrate as IMF come into effect in the range of nanometers. With regard to establishing this kind of intimate contact in the AFP process, the driving force provided by the compaction roller is assisted by both interfacial attractiveness and viscous flowability in order to effectively spread resin on the adherend surface. The contact formation of prepregs on different surfaces was recently studied by Choong et al. [16] who investigated contact evolution between prepreg and a glass substrate by optical microscopy as demonstrated before for PSA [17]. After exploring the relationship between the degree of intimate contact (DoIC) and tack, the authors concluded that the DoIC plays an important role, but its simple maximization turns out insufficient for process optimization. Instead, utilizing the superordinate tack curves is more appropriate and represents both the adhesive and cohesive phenomena governing prepreg tack.

This is the first research paper of a two-part series dealing with the adhesion-cohesion balance of prepreg tack and its relevance for automated fiber placement processes. For the present paper, the adhesive portion of the balance is covered by examining the fundamentals of bond formation between prepreg and different AFP-related contact materials.

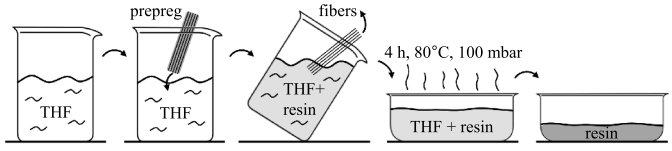

Fig. 2. Prepreg resin extraction procedure in tetrahydrofuran.

Therefore, a wetting analysis for prepregs is presented for the first time in literature allowing insight into the interfacial interaction governing adhesion. The wetting analysis is based on contact angle measurements between standard test liquids as well as extracted neat prepreg resin and solid substrate, namely stainless steel of different surface roughness, siliconized backing paper, polyurethane and the prepreg itself. Complementary optical characterization of the surface topographies is performed by laser scanning microscopy. Viscoelastic behavior of prepreg resin is examined by oscillatory rheology and results are used to test the validity of selected contact formation criteria for prepregs that have originally been developed for PSA. All findings from material analysis are discussed against the background of tack measured on a commercial carbon fiber-epoxy prepreg system in a probe tack test carried out in a rheometer. The two-phase design of the test procedure (compression to tension) enables to exclusively vary test parameters, which influence contact formation and therefore adhesion, while cohesion-relevant deformation parameters are kept constant. Strict separation of adhesive and cohesive contribution can thus be achieved and both portions investigated individually. The novel approach of this study aims at gaining fundamental insight into to the connectivity between interfacial resin-substrates interaction and macroscopic aspects involved in practical prepreg tack measurement.

2. Materials

2.1. Prepreg

The commercially available prepreg system Hexply 8552 [18] by Hexcel Corporation was used for all investigations and material characterization presented. The unidirectional aerospace-grade prepreg system is made up of AS4 carbon fiber and amine-cured epoxy resin featuring a nominal fiber volume fraction of 57.42 vol% and a nominal laminate density (cured) of 1.58 g/cm^3, respectively. The prepregs contain a thermoplastic toughener (~20 wt.% PES), which is initially miscible in uncured resin and forms a second phase upon curing for the toughening effect [19]. The recommended cure cycle is performed in an autoclave at 180 °C maximum temperature. 10 days tack life, 30 days out life and 12 months shelf life are guaranteed by the supplier according to data sheet.

2.2. Neat resin

Since formulation details and commercial availability of resin used for prepregs are strictly limited by material suppliers, neat resin had to be extracted from prepreg sheets by solvent extraction. Tetrahydrofuran (THF, >99.9%, BHT-inhibited) was used as a solvent for the extraction procedure shown in Fig. 2. THF is known to be an excellent solvent for epoxy resins and is thus commonly used as eluent for molecular weight analysis by gel permeation chromatography (GPC). After dissolving the prepreg matrix in THF at room temperature and removing the carbon fibers manually, the THF/resin solution was conditioned at 80 °C and 100 mbar over a period of 4 h to guarantee total solvent evaporation. The resin/toughener morphology and potential changes due to the presence of THF remain unknown. However, the solved state of the toughener is unlikely to change as all subsequent investigation and preparation take place prior to cure. THF evaporation was eventually assumed complete after 4 h of conditioning as the viscosity values of

Table 1
Investigated contact materials and their role in automated fiber placement processes.

Substrate		Occurrence in AFP	Abbreviation
Prepreg		Previously laid plies	PP
Backing paper		Protective film on prepreg	BP
Polyurethane		Compaction roller material	PU
Steel	ground	Mold material	ST
	polished	Mold material	ST_{pol}

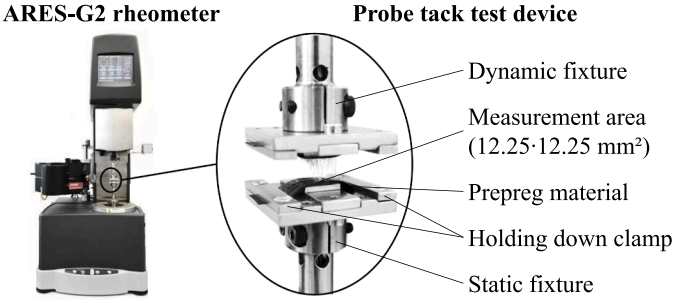

Fig. 3. Utilized equipment for prepreg tack measurement by probe tack testing.

extracted neat resin matched the data sheet (~500 Pa s at 60 °C and 1 Hz [18]). Untreated resin specimens as well as specimens that were comparatively treated for only 2 h showed significantly lower viscosity indicating residual solvent. In case of the 4 h samples, the risk of undesired cure reaction could be eased by DSC measurement, which showed no significant difference between cure peak enthalpies of fresh (486.3 J/g) and 4 h-conditioned (489.2 J/g) prepreg specimens (Appendix: Table A1). Hence, all results gained from material analysis including neat resins are assumed to be representative for the resin within the prepreg as delivered.

2.3. Contact materials

Prepreg tack and surface wetting is investigated on different substrates that are in contact towards prepreg material during fiber placement. Apart from using the commercial prepreg/backing paper substrates (Section 2.1) as delivered, a standard X5CrNi18–10 stainless steel is ground using SiC 80 grit grinding paper (ground specimens). The same steel is sequentially ground with 80, 120, 220, 500, 800, 1200 and 2000 grit SiC paper with a subsequent 3 and 1 μm diamond suspension polishing procedure to produce polished specimens. Polyurethane samples are fabricated by casting Sika Biresin U1404, a two-component, amine-crosslinked elastomeric casting resin, on a flat mold. The mold-facing sides of the samples are used for investigation due to higher planarity compared to the air-facing sides. Table 1 provides an overview of the examined substrates and their relevance in AFP.

3. Experimental methods and data analysis

3.1. Tack measurement

Tack measurement was performed as a probe tack test (compression to tension test) using a TA Instruments ARES G2 rheometer (Fig. 3). Prepreg material is clamped on a lower, static fixture which prevents the material from undesired detaching or bending. The upper fixture is attached to the axial servo control system of the rheometer enabling transient normal force measurements within an axial transducer range of 0.001–20 N. The dynamic upper fixture holding the probe is normally brought into contact with the prepreg until a distinctive pressure is built up, held (pressure-controlled) for a set dwell time and is eventually removed in an upwards direction at a controlled rate. The separation work W_{tack} defined as the energy needed to fully separate the sample interface during the tension phase is employed as an indicator for tack and calculated by integration of the stress strain curves. Throughout the whole procedure, precise temperature control (deviation ≤ 0.2 K) in the tack-relevant temperature range between 20 °C and 70 °C is guaranteed by a forced convection surrounding the specimen holders. The two-phase measurement cycle is presented in detail in [10] and allows to separately control the compression and tension phases. Therefore, testing parameters that influence adhesive bond formation/wetting process (compaction time and pressure) and those which determine cohesion upon debonding (debonding rate) can be investigated independently of each other. For this study, the latter is remained constant at 0.1 mm/s for all experiments. Compaction time and pressure are varied at increments of 5/10/15 N/cm^2 and 0.5/5/50 s, respectively. 10 N/cm^2 and 5 s of compaction are used as standard test parameters for all experiments without compaction variation. Three fresh prepreg samples were prepared and tested for each testing parameter to evaluate reproducibility as performed in our previous experimental study [10]. The variation range of the experimental compaction parameters does not fully represent actual process parameters of AFP (due to restrictions of the measurement device) as compaction pressure is usually higher and compaction time significantly shorter depending on the lay-up velocity and roller geometry. However, the large investigation range of the study is considered beneficial for getting an understanding of the fundamentals of prepreg resin surface wetting.

3.2. Wetting analysis

Liquid-solid interaction of neat epoxy resin and standard test fluids with different contact materials is carried out by three-phase contact angle measurement using a Kruess DSA25 Drop Shape Analyzer. The analytical apparatus includes the optional accessories of a temperature-controlled measurement chamber and syringe dosing unit to perform wetting experiments in the tack-relevant temperature range between 20 and 70 °C. The contact angle (CA) θ is estimated using the sessile drop technique and is related to the solid surface free energy σ_{SG}, solid/liquid interfacial free energy σ_{SL} and (liquid) surface tension σ_{LG} via Young's equation [20]:

$$\sigma_{SG} = \sigma_{SL} + \sigma_{LG} * \cos\theta \tag{1}$$

The surface free energies (SFE) as a quantitative measure of the intermolecular forces at the surfaces of the investigated contact materials are determined employing the method by Owens, Wendt, Rabel and Kaelble (OWRK, [21]). Here, the underlying interactions are divided into dispersive and polar portions represented by $\sigma^d_{SG}/\sigma^d_{LG}$ (dispersive) and $\sigma^p_{SG}/\sigma^p_{LG}$ (polar), respectively:

$$\sigma_{SL} = \sigma_{SG} + \sigma_{LG} - 2\sqrt{\sigma^d_{SG}\sigma^d_{LG}} - 2\sqrt{\sigma^p_{SG}\sigma^p_{LG}} \tag{2}$$

Substituting for σ_{SL} from Eq. (1) gives Eq. (3) in a linear form:

$$\underbrace{\frac{\sigma_{LG}(1+\cos\theta)}{2\sqrt{\sigma^d_{LG}}}}_{y} = \underbrace{\sqrt{\sigma^p_{SG}}}_{m} * \underbrace{\sqrt{\frac{\sigma^p_{LG}}{\sigma^d_{LG}}}}_{x} + \underbrace{\sqrt{\sigma^d_{SG}}}_{c} \tag{3}$$

A graphical representation of Eq. (3) can now be established by adding polar and dispersive surface tension (SFT) values of standard test liquids. For this study, analytical grade water and diiodmethane were used. SFT literature values for both standard liquids were verified by employing the pendant drop method at room temperature in an air atmosphere. The high viscosity of b-staged neat prepreg resin at room temperature prevented reproducible drop formation so that the measurement temperature needed to be increased. A temperature of 70 °C within the measurement chamber was found to be high enough for forming stable drops hanging from a needle (1.5 mm inner diameter) with a corresponding viscosity of 200 Pa s. The sessile drop experiments,

Table 2
Parameter set for the rheological analysis of neat epoxy prepreg resin.

Sweep	Temperature	Frequency	Strain
Temperature	**20 - 70 °C, linear: 5 K/min**	1 Hz	1%
Frequency	20 - 70 °C, 10 K increments	**10^{-2} – 10^{2} Hz log: 20 pts/dec**	1%
Amplitude	20 - 70 °C, 10 K increments	1 Hz	**10^{-2} – 10^{2}% log: 20 pts/dec**

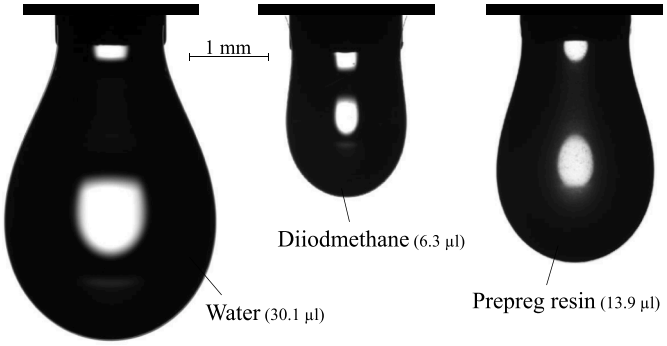

Fig. 4. Representative pendant drops of water, diiodmethane (room temperature) and prepreg resin (70 °C) hanging from a 1.5 mm blunt cannula for SFT determination.

including the extracted epoxy resin, were carried out at 70 °C as well. It was ensured that all wetting experiments were carried out within ~60 min after placing the resin syringes in the heated measurement device to avoid undesired resin cure.

3.3. Rheology

Viscoelastic characterization of neat prepreg resin won by the extraction procedure presented in Section 2.2 was performed as oscillatory rheometry utilizing the TA Instruments ARES G2 rheometer. Running a plate-plate configuration of 25 mm diameter, the complex viscosity η*, viscoelastic storage modulus G" and loss modulus G' as well as the equivalent loss factor tan δ were determined at 1 mm gap. Temperature, frequency and amplitude sweeps were carried out according to the testing parameters displayed in Table 2. The temperature increments for frequency and amplitude sweeps were reduced to 5 K/min within the highly-sensitive temperature range of prepreg tack between 30 and 50 °C.

3.4. Surface topography

The substrate topography is investigated optically using a Keyence 3D Laser Scanning Confocal Microscope VK-X. Root mean square roughness R_q of the ordinate value z(x) is determined within a sampling length l_r of 2.5 mm according to Eq. (4). Cutoff wavelengths in order to distinguish between roughness and waviness profiles are set according to the recommendations of ASME B46.1 [22]. Additionally, the maximum wavelength of each roughness profile λ_0 is determined for the experimental verification of a stickiness criterion. Five different locations on each substrate are measured in order to quantify standard deviation of the roughness parameters.

$$R_q = \sqrt{\frac{1}{l_r}\int_0^{l_r} z^2(x)\,dx} \tag{4}$$

Table 3
Total surface tension σ_{LG} as the sum of the polar σ^p_{LG} and dispersive σ^d_{LG} components of standard test liquids and extracted resin from HexPly 8552 prepreg. Literature values [23] and own data are given in mN/m.

Test liquid	Literature values			Pendant drop experiments		
	σ_{LG}	σ^p_{LG}	σ^d_{LG}	σ_{LG}	σ^p_{LG}	σ^d_{LG}
Water (20 °C)	72.8	51.0	21.8	72.31 ± 0.06	50.90 ± 0.55	21.41 ± 0.55
Diiodmethane (20 °C)	50.8	0.0	50.8	50.27 ± 0.36	0.47 ± 1.50	49.80 ± 1.46
Epoxy 8552 (70 °C)	–	–	–	39.74 ± 0.64	8.24 ± 1.26	31.50 ± 1.12

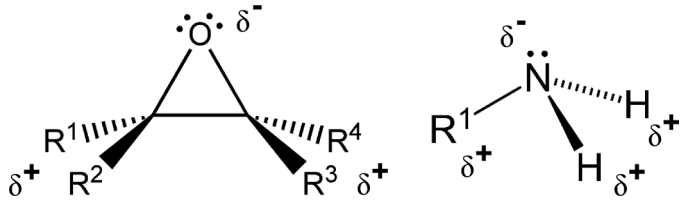

Fig. 5. Polarity of epoxide (left) and primary amine (right) groups due to high electronegativity of oxygen and nitrogen.

4. Results and discussion

4.1. Surface tension (SFT)

Pendant drop experiments were carried out to determine the surface tension of the test liquids water, diiodmethane and prepreg resin. The SFT values serve as the foundation for further interfacial wetting analysis. Fig. 4 shows representative drop shapes and sizes. With the help of a Young-Laplace fit of the optically determined drop geometries and the known test liquid densities, the total surface tensions σ_{LG} were calculated and summarized in Table 3. Polar and dispersive portions could be obtained from the liquid-solid interaction of the test liquids with the fully dispersive backing paper (Section 4.2). The SFT including its polar and dispersive component of both standard test liquids are in overall good agreement with the values presented in literature. The slight but significant deviation between SFT values from literature and own measurements (Table 3) is likely attributed to contamination during storage and test preparation. Especially for the total SFT of water, the difference between literature and own measurement (0.49 mN/m) is notable considering the low standard deviation of 0.06 mN/m . The surface tension of prepreg resin at 70 °C amounts to 39.74 mN/m with a polar portion of 20.73% equaling $\sigma^p_{LG} = 8.24$ and $\sigma^d_{LG} = 31.50$ mN/m, respectively. In contrast to the standard test liquids, the drop formation of the prepreg resin was highly influenced by viscoelastic behavior. However, dimensionally stable drops that ceased from deformation after a time span of approximately 60 s could be produced when dosing 14 µl resin from the syringe. The resin drops remained a Laplacean shape so that SFT could be calculated with the resin density of 1.2 g/cm^3. Overall, the findings for the resin SFT match the results presented Synytska et al. [24] who measured SFT by pendant drop experiments on two epoxy resins and amine hardeners. The SFT of the mixed systems were not measured directly but assumed to amount between both components (resins: 44.1 and 36.3 mN/m; hardeners: 35.7 and 33.3 mN/m). Wilhelmy experiments on bisphenol A diglycidyl ether (DGEBA) and tetraglycidyl methylene dianiline (TGMDA) performed by Page et al. [25] revealed SFT between 35 and 40 mN/m m^{-1}. No subdivision of SFT into polar and dispersive components were made in these studies.

Although the exact formulation of the commercial prepreg resin is unknown, a substantial share of polarity can be contributed to the presence of polar epoxide groups (Fig. 5, left) within the B-staged, partly cured resin. Here, the highly electronegative oxygen atom leads to

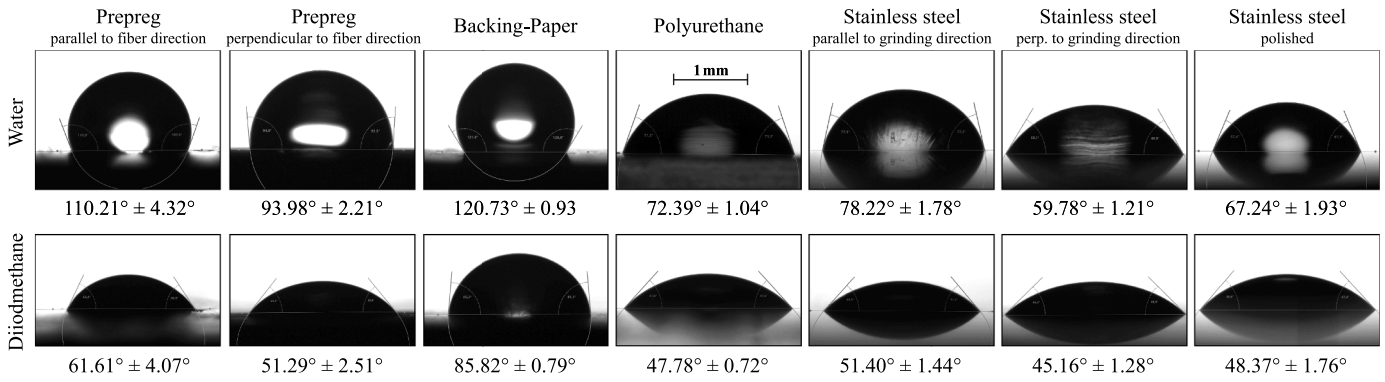

Fig. 6. Sessile drops (~2 µl) and their contact angles of water and diiodmethane on different AFP-related substrates. Seven drops were measured for each liquid/solid combination immediately after drop placement.

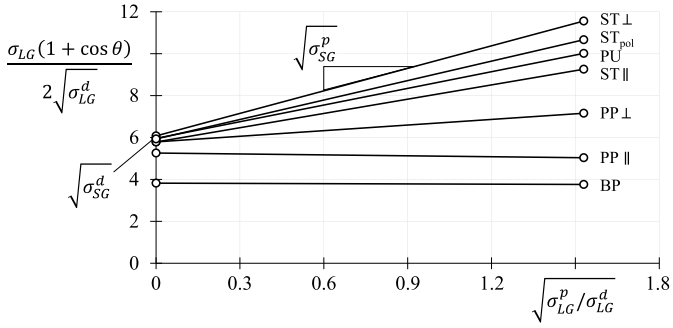

Fig. 7. Linear regressions for SFE determination according to the OWRK model.

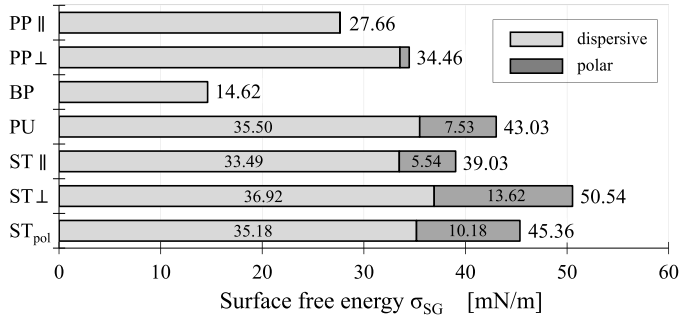

Fig. 8. Surface free energies σ_{SG} with their polar σ^p_{SG} and dispersive σ^d_{SG} components.

separation of charge and to an electric dipole moment. As the resin is amine-cured according to data sheet, a similar effect can be expected to result from the presence of amine groups (Fig. 5, right). Epoxy resin systems used for aerospace primary structures usually contain the 4,4′-diaminodiphenyl sulfone (DDS) as the hardener component in order to achieve a high glass transition temperature T_g (>160 °C) after autoclave cure [26]. The diamine-based hardener has a central sulfonyl group (*O=S=O*) which is highly polar measuring 4.5 Debye [27] and will most likely account for to the resin polarity as well. A more detailed insight into functional groups and their role for molecular polarity can be achieved by spectroscopic measurement techniques such as Fourier-transform infrared spectroscopy.

4.2. Substrate wetting analysis of standard test liquids

The substrate wetting analysis is based on three-phase contact angle measurement between the gaseous (air), solid (investigated substrates) and the liquid (water, diiodmethane, resin) phases with the SFT as presented in the previous section. Significant differences between the contact angles (CA) of the standard test liquids water and diiodmethane on the investigated substrates were observed as pictured in Fig. 6. Strong deviation from radial drop symmetry arose on surfaces with high directional surface topography as drops formed ellipsoidal shapes. As a consequence, divergent CA were measured on the same surfaces for different sample orientations. The phenomenon was most pronounced on the roughly ground stainless steel surface and on unidirectional prepreg which is why sessile drop formation was investigated parallelly and perpendicularly to the grinding/fiber direction on these surfaces. Detailed information on the direction-related differences in surface topography are provided in Section 4.6.

The wetting ability of water decreases in the order of increasing measured CA as follows: backing paper (BP), prepreg (parallel, PP∥), prepreg (perpendicular, PP⊥), ground stainless steel (parallel, ST∥), polyurethane (PU), polished stainless steel (ST$_{pol}$), ground stainless steel (perpendicular, ST⊥). As expected, water generally forms greater CA due to its higher SFT and specifically its notable polar component. Diiodmethane turned out to be a suitable fully dispersive test liquid as CA > 0° formed on all surfaces. The wetting order of diiodmethane slightly differs from the order observed for water, however, these differences are within standard deviation. The overall measured CA of the standard liquids range from the most likely silicone-coated backing paper (CA > 120° for water) to the perpendicularly ground stainless steel surface (CA ≈ 45° for diiodmethane). Applying the OWRK model to the CA measurement results, the linear regressions displayed in Fig. 7 can be calculated using Eq. 3.

By utilizing the model, the interfacial interactions are divided into dispersive and polar SFE components. As the graph slopes represent the square root of the polar SFE components, a horizontal line signals a fully dispersive surface with evanescent polar contribution. The dispersive component can be read directly from the ordinate measuring the square root of the dispersive component. The SFE compositions of the investigated substrates are displayed in Fig. 8. The polished and perpendicularly ground stainless steel substrates show the highest total SFE values followed by PU and ST∥. For these substrates, polar portions between 14.19% and 26.95% were measured. The siliconized backing paper exhibits an extremely low, fully dispersive SFE of 14.62 mN/m. Despite its strongly polarized -(Si-O)- backbone, outside methyl groups shield polarity which results in a fully dispersive surface with excellent release properties. The polar portion of the prepreg SFE were also found to be near zero and therefore, lower than the SFT polar portion of neat resin. Reasons for this discrepancy may be exposed non-polar carbon fibers on the prepreg surface or small amounts of solvent residue in the resin from the extraction process. SFE on the roughest surfaces (PP and ST, see Section 4.6) were generally lower if measured in a parallel orientation to the fiber/grinding direction. This observation is most likely caused by enhanced flowability of the test liquids along grooves due to capillarity.

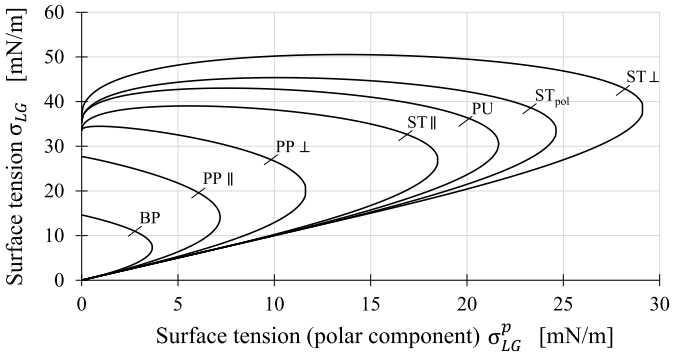

Fig. 9. Wetting envelopes for fully spreading liquids (θ = 0°) based on the OWRK model.

The drop spreads elliptically in fiber/grinding direction and, for this test setup, leads to higher contact angles and lower SFE, respectively.

Wetting envelopes are a useful type of exemplification whenever liquids are to be modified in order to achieve desired wetting properties on surfaces with known SFE. For prepreg resins, they can reveal possibilities of resin modification in the material development phase in terms of the polar-to-dispersive SFT ratio. Fig. 9 shows the wetting envelopes of the investigated surface materials for full drop spreading (CA = 0°). Liquids with $\sigma_{LG}/\sigma^p_{LG}$ pairs of values, that are located within the envelopes, will fully wet the corresponding surface. The sizes of the wetting envelopes unsurprisingly follow the same order as the wetting ability of the standard test liquids presented Fig. 6. Complete spreading of liquids on backing-paper will exclusively be observable for liquids with extremely low SFT such as perfluorohexane (~12 mN/m).

4.3. Surface wetting of viscous prepreg resin

While characterizing the wetting behavior of the low-viscosity standard test liquids diiodmethane and water turned out unconditionally, restrictions had to made concerning the contact angle measurements of the extracted prepreg resin. On the one hand, the resin was not dosable from the syringe below temperatures of 70 °C due to high viscosity (> 200 Pa s). On the other hand, pronounced viscoelastic behavior led to strong time-dependent deformation of the sessile resin drops after drop placement. The dynamics of viscous liquids on rigid surfaces in general and its quantification by contact angle measurement in particular are a special matter of liquid/solid interaction. The issue has been attended to by advancing and receding contact angle measurement in literature [28–30]. Fig. 10 shows the evolution of contact angles on the investigated substrates as a function of time. The resin drop CA exponentially decreases on all substrates until finally reaching a threshold. The threshold value is reached after 180 s for all substrates excluding the prepreg surfaces in both directions. Viscoelastic relaxation of stresses induced during drop placement influences the three-phase equilibrium state of the drops and is therefore considered the driving force of time-dependent CA evolution. Also, time-dependent mechanisms, in which polymer chains are rearranged and polar groups exposed at the interface have been reported in literature [31] and most likely contribute to the observations as well. On prepreg, the resin continuously spreads and reaches close to complete spreading within the investigated time range. It is assumed that a drop of prepreg resin on a prepreg surface at elevated temperatures cannot be treated as a model system of three ideally separated phases. The prepreg surface (excluding the contribution of the carbon fibers) is in a viscous state and creates a semi-solid interface which is most likely dominated by autohesion/self-diffusion mechanisms.

For all following calculations involving the contact angles of resin drops, the CA values in the equilibrium stage after 180 s are utilized. The spreading coefficient (SC) can be expressed as the difference between surface tension/energy σ_{SG}/σ_{LG} and the interfacial tension σ_{SL}:

$$SC = \sigma_{SG} - (\sigma_{LG} + \sigma_{SL}) \quad (5)$$

In Fig. 11, spreading coefficient isolines are drawn for prepreg resin as a function of both dispersive and polar SFE components. gray dots indicate the measured SFE value pairs for the investigated substrates. According to the simple relationship of Eq. (5), it appears that wetting is favored by a low interfacial free energy, a high solid surface energy and a low liquid surface tension. Negative spreading coefficients will give a measurable CA > 0° The OWRK model using standard test liquids predicts complete drop spreading (SC < 0; CA = 0°) for prepreg resin on polyurethane and stainless steel. These predictions were not fully

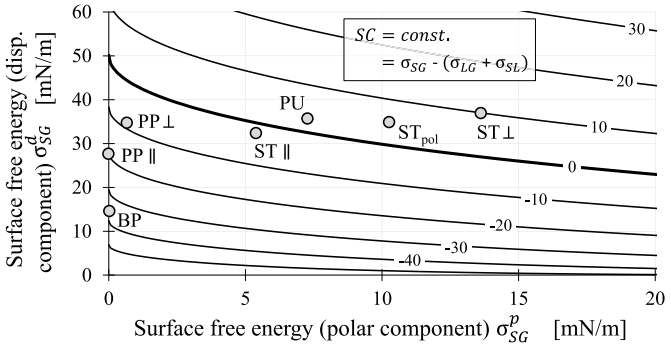

Fig. 11. Spreading coefficient SC [mN/m] isolines for prepreg resin (70 °C) as a function of polar and dispersive SFE components.

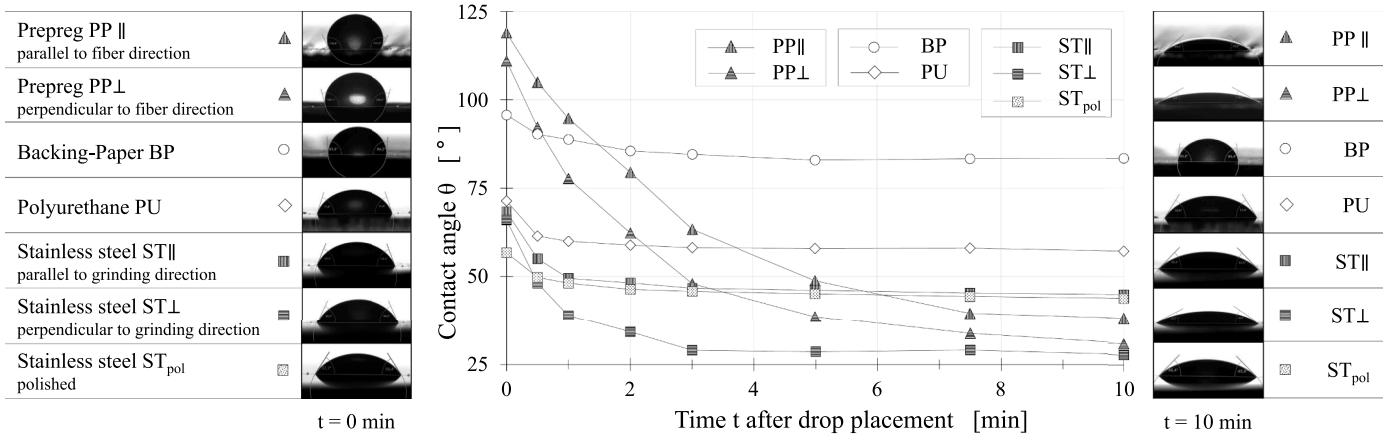

Fig. 10. Evolution of prepreg resin drops on different substrates over a time span of 10 min (right) after drop placement (left).

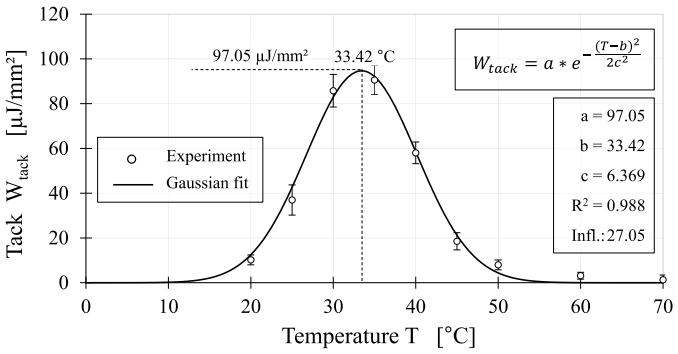

Fig. 12. Experimental data and Gaussian model fit of tack between two prepreg plies as a function of temperature. The data is obtained for standard test parameters of 10 N/mm^2 compaction pressure and 5 s compaction time.

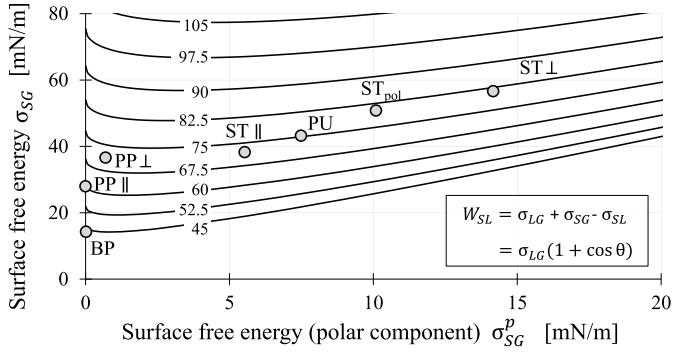

Fig. 13. Thermodynamic work of adhesion W_{SL} [mN/m] isolines as a function of polar and dispersive SFE components.

supported by the measured CA presented in Fig. 10 as threshold CA > 0° were observed on all surfaces. However, CA were significantly smaller and matched the model-predicted order - with the exception of the prepreg surfaces due to diffusion being the dominant contact mechanism. In terms of topographical anisotropy, the significant differences between PP∥ and PP⊥ as well as ST∥, ST⊥ and ST_{pol} cannot be explained by chemical factors as these surfaces are obviously identical in terms of chemical composition. The different wetting behavior is therefore rather a matter of flowabilty and surface topography which is why an additional analysis of both factors was performed (Sections 4.5 and 4.6).

4.4. Role of adhesive attraction for prepreg tack

In an effort to test the hypothesis that the thermodynamic work of adhesion determines the adhesive attraction and, eventually correlates with the tack of prepregs in the adhesive regime, tack measurements were performed for the contact materials utilizing the probe tack test in a rheometer. The measured data was fitted by Gaussian curves as done by Choong [16], Smith [6] and Endruweit [32]. As pointed out by the authors, the Gaussian fit is a purely phenomenological fit and lacks physical representation. However, the model fit enables the calculation of curve characteristics such as maximum tack and tack onset as a function of temperature as the independent variable. The Gaussian fit of temperature-dependent tack between two prepreg plies as well as its corresponding experimental results are plotted in Fig. 12. Here, the fit parameter *a* represents the maximum tack at the temperature *b*, while *c* determines the slope shape and therefore the sensitivity of prepreg tack to temperature deviation. The temperature of 27.05 °C marks the first inflection of the Gaussian fit where dW_{tack}/dT is maximum in the adhesive regime (left side of the bell-shaped curve). For this study, it will be regarded as the onset temperature of tackiness T_{onset} at which

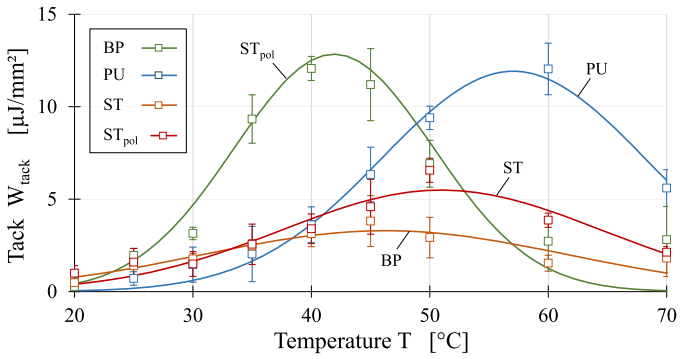

Fig. 14. Temperature-dependent tack for different surface combinations utilizing the probe tack test.

bonding is controlled by interfacial adhesion between resin and substrate. The corresponding failure mechanism is adhesive failure and is indicated by the absence of resin residue on the contact material. In this context, the thermodynamic work of adhesion W_{SL} is a measure of the strength of the contact between two phases [33]. W_{SL} is defined as the reversible thermodynamic work required to separate the interface from the equilibrium state of two phases to a separation distance of infinity [34]. It amounts to the difference between the released energies due to the respective surface tensions of σ_{LG}/σ_{SG} and the depleted interfacial tension σ_{SL} when forming a new liquid-solid interface. It is closely related to the spreading coefficient (Eq. (5)) and is calculated as follows:

$$W_{SL} = \sigma_{LG} + \sigma_{SG} - \sigma_{SL} \quad (6)$$

Fig. 13 shows the investigated surface materials as a function of SFE and their classification between W_{SL} isolines. Based on the surface wetting analysis and the herein determined model-based work of adhesion alone, prepreg tack - at least in the low temperature, adhesive fracture regime - is expected to increase in the following order: BP, parallel, PP∥), prepreg (perpendicular, PP⊥), ground stainless steel (parallel, ST∥), polyurethane (PU), polished stainless steel (ST_{pol}), ground stainless steel (perpendicular, ST⊥). Tack between prepreg-prepreg specimens is expected to be highest due to intermolecular entanglement as a result of self-diffusion during the compression phase (see discussion in Section 4.3). Fig. 14 shows the probe tack curves of prepreg for different surfaces as a function of temperatures. Again, experimental data and fitted Gaussian curves are presented. Generally, prepreg tack towards the investigated solid substrates is found to be significantly lower (roughly one magnitude) than between two prepreg sheets. Similar results were reported by Endruweit et al. [32] and Crossley et al. [35]. A significant difference in tack of prepregs towards different contact materials was also observed by Choong et al. [16] who measured maximum tack force of 42.41 ± 1.66 N for prepreg-prepreg and 5.07 ± 0.53 N for prepreg-steel. All aforementioned authors used a continuous application-and-peel procedure which has recently been standardized in ASTM D8336–21 [36].

Comparing the model with the experimental probe tack curves of different substrates reveals that the aforementioned model-predicted order is not fully supported as the thermodynamic work of adhesion W_{SL} apparently does not exclusively determine the adhesive portion of prepreg tack. This becomes most evident for the steel substrates that differ greatly in both maximum tack and the corresponding temperature despite the similar W_{SL} of 78.47 and 84.90 mN/m. Also, polyurethane is located in the same range in terms of W_{SL} and adheres significantly better than ground steel. The lowest measured tack towards backing paper was anticipated in view of the facts that the absolute W_{SL} is lowest (42.96 mN/m) and its polar/dispersive SFE component ratio (fully dispersive) matches the ratio of prepreg resin (20.73%) least. Comparing the ratios between the polar and the dispersive portion of the SFT of liquids and the SFE of solids generally enables an assessment of

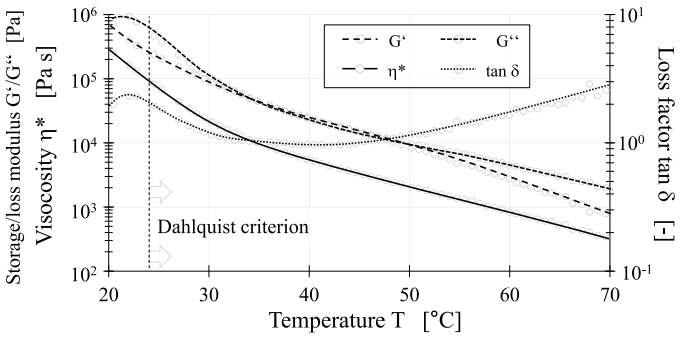

Fig. 15. Viscoelastic parameters of extracted prepreg resin within the tack-relevant temperature range.

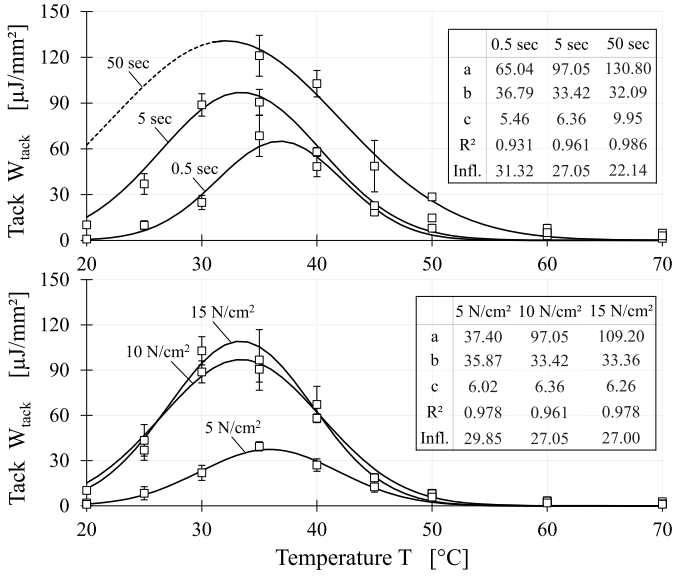

	0.5 sec	5 sec	50 sec
a	65.04	97.05	130.80
b	36.79	33.42	32.09
c	5.46	6.36	9.95
R^2	0.931	0.961	0.986
Infl.	31.32	27.05	22.14

	5 N/cm²	10 N/cm²	15 N/cm²
a	37.40	97.05	109.20
b	35.87	33.42	33.36
c	6.02	6.36	6.26
R^2	0.978	0.961	0.978
Infl.	29.85	27.05	27.00

Fig. 16. Tack between two prepreg plies as function of compaction time (upper graph), compaction pressure (lower graph) and temperature. The dashed line for 50 s compaction was extrapolated due to reaching the load restriction of the test apparatus.

adhesion: The better the ratios coincide, the more interaction can be expected possible between the involved phases. The low, fully dispersive interaction of the prepreg resin towards backing paper is exclusively dominated by van der Waals forces which result from temporary fluctuations of the charge distribution (London dispersion forces). The interactions of the other surfaces include a polar portion that increases the thermodynamic work of adhesion and presumably leads to the formation of intermolecular hydrogen bonds between resin and substrate. Although higher W_{SL} at the interface appears to lead to higher absolute tack, the wetting analysis based on contact angle measurement cannot fully clarify all substrate-related differences in prepreg tack including the temperature-shifts and the exact order of increasing tack. Thus, additional rheological analysis was performed to investigate its contribution to the wetting process.

4.5. Rheological implication in resin surface wetting

Characteristic viscoelastic parameters of neat prepreg resin, namely complex viscosity η*, storage modulus G', loss modulus G" and its ratio the loss factor tan δ, are given in Fig. 15 as a function of temperature for a frequency of 1 Hz and 1% strain. The decrease in viscosity extends to three magnitudes within the examined temperature range. Questions arise as to when the viscosity is low enough for the prepreg resin to

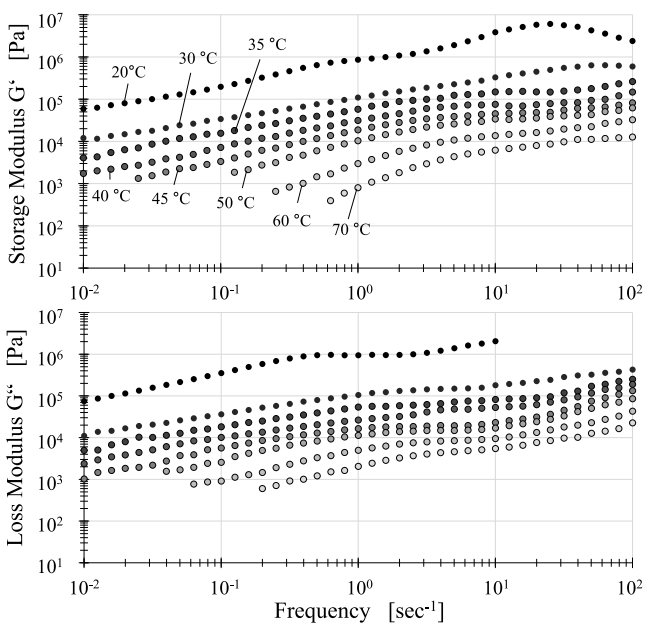

Fig. 17. Frequency-dependent viscoelastic moduli G' and G". Data for low frequencies and high temperatures is not shown due to high fluctuation in this region. Here, curve smoothing was performed by average determination of five adjacent data points.

sufficiently wet a substrate which would mark the onset of measurable tackiness. The presumably most prominent criterion to estimate the adhesive reliability of soft polymers on rigid substrates, that means to determine whether a viscoelastic material is contact efficient or deficient, is the Dahlquist criterion [37]. Although this criterion is limited to the single characteristic viscoelastic value of G' < 0.3 MPa, it has shown remarkable universality across different kinds of PSA and substrates. Crossley et al. [9] tested the Dahlquist criterion's applicability for epoxy prepregs using a single-stage peel test for different hand lay-up prepregs. Although the general criterion principle was found valid, it was assumed by the authors that the criterion is rather a function of prepreg and mold surface conditions. Examining the viscoelastic analysis in this paper, the G' curve of extracted prepreg resin crosses the 0.3 MPa Dahlquist line at 23.8 °C (Fig. 15). Meanwhile, T_{onset} for the prepreg-prepreg surface combination amounts to 27.05 °C (Fig. 12) with a corresponding G' of 0.16 MPa. This finding is considered a decent agreement with the Dahlquist criterion for this particular material combination. However, the limitations of the Dahlquist criterion for prepreg tack become apparent when consulting the tack results as a function of the contact relevant test parameters compaction time and compaction pressure displayed in Fig. 16. The dependence of T_{onset} on the compaction parameters indicates that the Dahlquist criterion can only be regarded as a rule of thumb rather than as a clear-cut value independent from further factors. As expected, an increase in both compression parameters leads to a shift of the maximum tack (fit parameter *b*) and tack onset (Infl.) towards lower temperatures. Furthermore, higher absolute tack is measured likewise which has repeatedly been reported in literature for different measuring techniques [5].

A more sophisticated evaluation of the role of viscoelasticity for tack performance of PSA was made by Chang [38]. According to Chang's proposal, tack-relevant application takes place within the frequency range of 10^{-2} Hz (creep) to 10^{2} Hz (peel). The corresponding viscoelastic moduli in this frequency range are shown in Fig. 17 for different temperatures. Consulting Chang windows for tack characterization of adhesives and resins does not exclusively focus on the wetting process but includes the debonding behavior as well [39]. This way, a categorization of tack performance (e.g. removable, high shear etc.) can be realized resting upon viscoelastic behavior. The windows are spanned

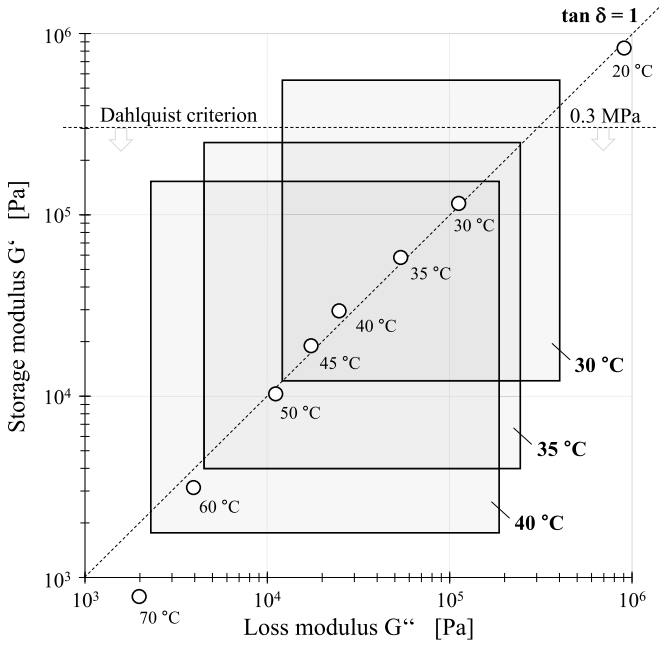

Fig. 18. Chang windows of neat prepreg resin for different temperatures.

within four corner points that are defined by the frequency-dependent G'/G" pairs of values at $10^{-2}/10^{-2}$, $10^{-2}/10^{2}$, $10^{2}/10^{-2}$ and $10^{2}/10^{2}$ Hz. Based on the data shown in Fig. 17, Chang windows were constructed by this procedure for selected temperature levels in Fig. 18. 1 Hz results (white dots) for all temperature levels are located near the G'/G" cross-over line (tan δ = 1) that separates the two regions of elastically and viscously dominated behavior. The closer a dot or a constructed viscoelastic window is located towards the top-left hand corner of the plot, the better removable the adhesive will be with an adhesive failure mechanism. Conversely, a location near the lower right hand corner of the plot will result in a more viscous, cohesively breaking material. The displayed Chang windows of 30, 35 and 40 °C are actually the only investigated temperature levels whose windows can fully be constructed within the storage and loss modulus range between 10^3 and 10^6 Pa. Remarkably, these are the medium temperature levels exhibiting maximum tack between two prepreg plies (see Fig. 12). Higher temperatures push the windows towards lower moduli while the low temperature window of 20 °C exceeds the graph towards higher moduli. According to our measurement at ~1 Hz, the highest tack levels for the prepreg-prepreg combination can be achieved when the Chang window of prepreg resin is located in the range of a 'general purpose PSA' (G' and G" roughly between 10^4 and 10^5 Pa) with a slight tendency towards higher moduli which corresponds to moderately lower temperatures. Based on this finding, adjusting a resin storage modulus G' of 10^4 Pa (at material deposition temperature) in the b-staging process is recommended if maximum tackiness is required in AFP.

In general, the Chang windows for prepreg resin appear significantly wider than the majority of Chang windows reported in PSA research [40–42]. Following the construction process of these viscoelastic windows, this is evidently observable due to a stronger frequency dependence of the viscoelastic parameters for epoxy prepreg resin than for most PSA formulations. Reasons are most likely that PSA design is performed to meet specific application requirements (clean removable, high resistance etc.) [43]. Meanwhile, rather the mechanical properties in combination with the reinforcement fibers are deciding for prepreg resin formulation. Considering the implication for practical use in advanced composite manufacturing, the results substantiate the challenging aspects of process adjustment: On the one hand, the high temperature- and frequency-dependence, and therefore large Chang windows, give processors the possibility of adjusting the lay-up process in a wide spectrum. This is beneficial if different tack levels are needed at different stages in the process, e.g., during material feeding/cutting and deposition. On the other hand, precise temperature control of the laid prepreg is mandatory and practically challenging, especially under special process conditions such as variable lay-up speed, complex geometries etc. [44].

No amplitude sweeps are presented here as no significant influence of the oscillatory deformation stress could be determined within the investigated measurement range for temperatures ≥ 35 °C. Hence, the limit of the linear viscoelastic region (LVE region) was not reached for these temperatures and plateau values could be determined. For lower temperatures near room temperature, repeated downturns of the moduli curves were observed indicating brittle fracturing behavior of the prepreg resin sample for high stresses outside the LVE region.

4.6. *Roughness-extended Dahlquist criterion*

Both criteria shown in the previous section are exclusively based on the viscoelastic behavior of the prepreg resin and therefore independent from contact material properties such as surface free energy and topography despite their apparent implication in prepreg tack. Fig. 19 shows topographic images of the contact materials taken by a 3D laser scanning confocal microscope. Non-contact optical measurement turned out to be the only suitable way to analyze the surface of uncured epoxy prepregs topographically. With the scale being normalized for comparison reasons, it becomes evident that the investigated surfaces differ greatly in terms of roughness. The order of round mean square roughness R_q (Eq. (4)) is determined as PP > PU > ST > BP > ST_{pol}. In contrast to structural adhesives, rougher surfaces are known decrease the adhesive performance of PSA [45]. For this type of bonding, deviations from an ideally smooth surface result in an increased potential contact area but will at the same time hinder the wetting process of viscous liquids [46]. The observation that surface conditions play an important role in PSA adhesion has eventually led to repeated refinement of the Dahlquist criterion in literature. In this context, Ciavarella and Papangelo [47] proposed an extended criterion incorporating surface topography based

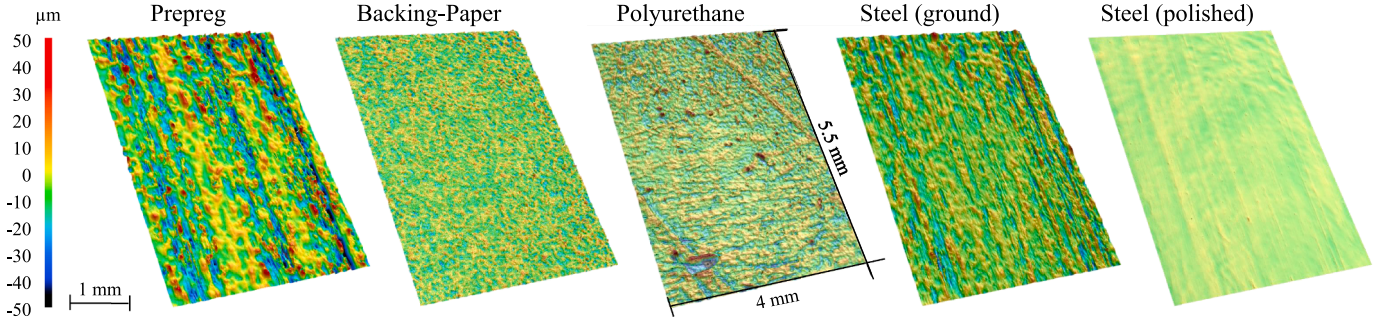

Fig. 19. Surface topographies of the investigated contact materials. Pictures were taken by 3D laser scanning microscopy (2.5x) and scale was normalized.

Table 4
Gaussian model fit parameters and characteristic value. Arithmetic mean values of R_q, λ_0 and W_{SL} are used for surfaces with significant influence of grinding/fiber direction (prepreg and ground steel). The OWRK-based surface polarities are given for comparison reasons with the resin polarity (20.73%).

Surface material	R_q [μm]	λ_0 [μm]	W_{SL} [mN/m]	G'_c [MPa]	T_c [°C]	T_{onset} [°C]	T_{max} [°C]	Polarity [%]
Prepreg	11.62 ± 2.16	39.7 ± 0.41	59.61 ± 3.42	0.005	53.9	27.05	33.42	0
Backing-paper	2.47 ± 0.38	17.9 ± 0.27	42.96 ± 0.61	0.031	38.2	30.79	46.22	0
Polyurethane	7.41 ± 0.53	50.1 ± 1.33	82.63 ± 0.64	0.019	42.1	45.97	57.05	17.49
Steel (ground)	2.04 ± 0.26	25.3 ± 0.65	83.93 ± 1.22	0.128	28.0	37.49	50.99	20.57
Steel (polished)	0.51 ± 0.06	31.3 ± 0.49	84.90 ± 1.33	2.554	11.2	33.51	41.91	22.44

on a generalized Johnson parameter. Topographical surface characteristics are represented by the root mean square roughness R_q and the maximum wavelength in the roughness profile λ_0 which are then combined with the thermodynamic work of adhesion W_{SL} as per:

$$G'_c = \frac{W_{SL}\ \lambda_0}{4\ {R_q}^2} \tag{7}$$

The simple relationship postulates that high adhesive attraction (represented by W_{SL}) and high wavelength will result in high critical moduli G'_c while rougher surfaces need low modulus liquids in order to achieve proper surface wetting. Utilizing the rheological data of Fig. 17, a corresponding critical temperature T_c can be determined for G'_c. At this specific temperature, the prepreg resin will fill the surface cavities (equaling a high degree of intimate contact) which should in theory result in a considerable increase in tack. Dahlquist and other authors did not specify in detail, when a PSA is to be considered contact efficient, e.g., as defined by a specific measurable tack level or degree of intimate contact. Hence, we define the first inflection point of the bell-shaped tack curves as the onset temperature of a considerable level of tackiness T_{onset}. (Section 4.4). It can be calculated from the Gaussian fits of the temperature-dependent tack curves presented in Fig. 14. Table 4 sums up the experimental topographical results and the calculated criterion-relevant contact parameters. As probe tack experiments are carried out perpendicularly towards the sample surfaces, different fiber/grinding directions cannot be respected. The G'_c values for PP and ground ST are therefore calculated by using the arithmetic mean values of R_q, λ_0 and W_{SL} for both directions.

Comparing the experimentally determined T_{onset} to the criterion-based T_c reveals basic applicability of the criterion to prepreg tack: The smooth surface of the polished steel specimens combined with high W_{SL} at the interface, e.g., leads to the highest modulus and therefore requires only low temperatures in order to guarantee sufficient surface wetting. The rougher ground steel surface with similar W_{SL} and λ_0 starts adhering at higher temperatures as predicted by the criterion. The medium roughness in conjunction with low W_{SL} of the backing paper leads to a medium modulus. However, the T_c of ST and BP appears less meaningful due to the less pronounced dependence of tack on the temperature (Fig. 14). In summary, the criterion is able to serialize the investigated surface materials in terms of a prepreg resin temperature that is necessary for surface wetting. The theoretical succession was generally supported by tack measurement except for the prepreg-prepreg combination (see Section 4.3 for discussion). However, the absolute values of T_c and T_{onset} differ significantly. There are several aspects that may be causing the difference:

- A potential temperature-dependency of the resin wetting process, which may influence W_{SL}, could not be accounted for in the wetting analysis because the viscous prepreg resin did not form stable drops for temperatures < 70 °C.
- The resin surface of the prepreg, which serves as the adhesive in the tack tests, is comparatively rough by itself ($R_q = 11.62$ μm) while only the roughness of the adherend was considered for the criterion.
- The anisotropy of the surfaces could not be respected for tack measurement, which is why calculation of T_{onset} is based on arithmetic mean values.
- Prepreg tack is subject to a variety of influencing factors [5]. The displayed results are only representative of a single set of testing parameters. The results presented in Fig. 16 illustrate that test parameter variation can cause shifts in the temperature spectrum.
- Compaction pressure and time are not considered by the criterion.
- In general, the validation procedure of the topographically extended Dahlquist criterion as performed in this study is very sensitive to deviation and measurement uncertainty. A slight difference in the estimated critical modulus G_c will, for example, result in a relatively large temperature shift due to the pronounced G' dependency on resin temperature.

5. Conclusion

In this paper, unidirectional carbon fiber prepreg was investigated in terms of probe tack and the interfacial interaction towards different AFP-related contact materials. Emphasis was placed on the bonding process by examination of the influence of surface wetting, rheology and topography. The results elucidate the fundamental mechanisms for contact formation and its role for measurable prepreg tack in the adhesive regime of the temperature-sensitive adhesion-cohesion balance. The key findings can be summarized as follows:

- Contact angle measurement in combination with the OWRK model proved to be a suitable approach to reveal significant differences in surface wetting of prepreg resin as well as standard test liquids on solid surface materials that are present in AFP.
- Contact formation between two prepreg plies cannot be treated as model system of three ideally separated phases and is therefore not approachable through CA measurement. For this material combination, adhesion is rather provided by autohesion mechanisms which eventually entail higher measurable tack than prepregs show towards solid substrates.
- High adhesive attraction between prepreg resin and a solid surface (represented by thermodynamic work of adhesion W_{SL}) favors higher tack values. However, the relation is found not to be straightforward as, e.g. differences in tack are found between steel surfaces of different surface roughness despite similar W_{SL}.
- Higher tack can be achieved on substrates with matching polar and dispersive SFT/SFE ratios. This way, both dispersive (van der Waals forces) and polar (h-bonding, dipole-dipole-interaction) can come to fruition at the interface.
- Rheological approaches to surface wetting and tack performance developed for pressure sensitive adhesives (PSA) proved to be basically applicable for thermoset prepregs but could not explain surface-related wetting phenomena in its entity. Variation of contact-relevant test parameters and contact materials could exemplify the limitations of these criteria.
- A topographically extended version of the Dahlquist criterion was successfully applied to investigate the implication of W_{SL}, surface topography and rheology in the temperature-dependent onset of tack in the adhesive failure regime via an estimated critical storage modulus G'_c. Although, absolute temperatures determined by tack measurement did not exactly match the criterion-predicted temperatures, the basic dependencies could be verified: While high W_{SL} and

large wavelengths in the roughness profile promote low temperature wetting, higher resin temperatures/lower storage moduli are required to thoroughly wet rough surfaces and, eventually, promote adhesion.

CRediT authorship contribution statement

D. Budelmann: Conceptualization, Methodology, Validation, Formal analysis, Investigation, Writing – original draft, Writing – review & editing. **C. Schmidt:** Conceptualization, Resources, Writing – review & editing, Supervision, Funding acquisition. **D. Meiners:** Conceptualization, Resources, Writing – review & editing, Supervision, Project administration, Funding acquisition.

Declaration of Competing Interest

The authors declare that they have no competing financial interests or personal relationships associated with this publication.

Acknowledgements

The authors would like to acknowledge the financial support by Deutsche Forschungsgemeinschaft (DFG – German Research Foundation) granted for the research project 'TackTIC – Tack of Thermoset Impregnated Carbon Fibers' (project number 458900231).

Appendix

Table A1

Table A1
DSC and rheological data of the extracted THF/resin mixture after different times of conditioning at 80 °C and 100 mbar.

	DSC		Viscosity at 60 °C/1 Hz [Pa s]	
Conditioning time [h]	T_{onset} [°C]	Cure enthalpy [J/g]	Neat resin (datasheet [18])	Measurement
0	124.3	486.3	500	131
2	123.6	488.9	–	384
4	125.6	489.2	–	493

References

[1] A. McIlhagger, E. Archer, R. McIlhagger, P.E. Irving, C. Soutis, Manufacturing processes for composite materials and components for aerospace applications. Polymer Composites in the Aerospace Industry, Elsevier, Amsterdam, 2015, pp. 53–75.
[2] S. Sun, Z. Han, H. Fu, H. Jin, J.S. Dhupia, Y. Wang, Defect characteristics and online detection techniques during manufacturing of FRPs using automated fiber placement: a review, Polym 12 (2020) 1337, https://doi.org/10.3390/polym12061337.
[3] P.D. Juarez, K.E. Cramer, J.P. Seebo, Advances in in situ inspection of automated fiber placement systems, in: Proc. SPIE 9861, Thermosense: Thermal Infrared Applications XXXVIII 986109, 2016, https://doi.org/10.1117/12.2223028.
[4] B. Denkena, C. Schmidt, K. Völtzer, T. Hocke, Thermographic online monitoring system for automated fiber placement processes, Compos. Part B 97 (2016) 239–243, https://doi.org/10.1016/j.compositesb.2016.04.076.
[5] D. Budelmann, C. Schmidt, D. Meiners, Prepreg tack: a review of mechanisms, measurement, and manufacturing implication, Polym. Compos. 49 (2020) 3440–3458, https://doi.org/10.1002/pc.25642.
[6] A.W. Smith, A. Endruweit, G.Y.H. Choong, D.S.A. De Focatiis, P. Hubert, Adaptation of material deposition parameters to account for out-time effects on prepreg tack, Compos. Part A 133 (2020), 105835, https://doi.org/10.1016/j.compositesa.2020.105835.
[7] A.M. Gillanders, S. Kerr, T.J. Martin, Determination of prepreg tack, Int. J. Adh. Adh. 1 (1981) 125–134, https://doi.org/10.1016/0143-7496(81)90035-X.
[8] K.J. Ahn, J.C. Seferis, T. Pelton, M. Wilhelm, Analysis and characterization of prepreg tack, Polym. Compos. 13 (1992) 197–206, https://doi.org/10.1002/pc.750130308.
[9] R.J. Crossley, P.J. Schubel, N.A. Warrior, The experimental determination of prepreg tack and dynamic stiffness, Compos. Part A 43 (2012) 423–434, https://doi.org/10.1016/j.compositesa.2011.10.014.
[10] D. Budelmann, H. Detampel, C. Schmidt, D. Meiners, Interaction of process parameters and material properties with regard to prepreg tack in automated lay-up and draping processes, Compos. Part A 117 (2019) 308–316, https://doi.org/10.1016/j.compositesa.2018.12.001.
[11] C. Creton, Pressure-sensitive adhesives: an introductory course, MRS Bull. 28 (2003) 434–439, https://doi.org/10.1557/mrs2003.124.
[12] I. Benedek, Pressure-Sensitive Adhesives and Applications, 2nd ed., CRC Press, New York, 2004.
[13] A.V. Pocius, Adhesion and Adhesives Technology, 3rd ed., Carl Hanser, Munich, 2012.
[14] Z. Czech, K. Wilpiszewska, B. Tyliszczak, X. Jiang, Y. Bai, L. Shao, Biodegradable self-adhesive tapes with starch carrier, Int. J. Adh. Adh. 44 (2013) 195–199, https://doi.org/10.1016/j.ijadhadh.2013.03.002.
[15] L.-.H. Lee, The chemistry and physics of solid adhesion, in: L.-H. Lee (Ed.), Fundamentals of Adhesion, Springer, Boston, 1991, pp. 1–75.
[16] G.Y.H. Choong, A. Endruweit, D.S.A. De Focatiis, Analysis of contact area in a continuous application-and-peel test method for prepreg tack, Int. J. Adh. Adh. 107 (2021), 102849, https://doi.org/10.1016/j.ijadhadh.2021.102849.
[17] C. Creton, L. Leibler, How does tack depend on time of contact and contact pressure? J. Polym. Sci. B Polym. Phys. 34 (1996) 545–554, https://doi.org/10.1002/(SICI)1099-0488(199602)34:3<545::AID-POLB13>3.0.CO;2-I.
[18] Hexcel Corporation, HexPly 8552, Epoxy Matrix (180°C/356°F Curing Matrix), Stamford, 2020.
[19] J.M. Faulstich de Paiva, A. De Nadai dos Santos, M.C. Rezende, Mechanical and morphological characterizations of carbon fiber fabric reinforced epoxy composites used in aeronautical field, Mater. Res. 12 (2009) 367–374, https://doi.org/10.1590/S1516-14392009000300019.
[20] T. Young, An essay on the cohesion of fluids, Phil. Trans. R. Soc. 95 (1805) 65–87, https://doi.org/10.1098/rstl.1805.0005.
[21] D.K. Owens, R.C. Wendt, Estimation of the surface free energy of polymers, J. Appl. Polym. Sci. 13 (1969) 1741–1747, https://doi.org/10.1002/app.1969.070130815.
[22] A.S.M.E. B46.1 –2019, Surface Texture (Surface Roughness, Waviness, and Lay), American Society of Mechanical Engineers, New York, 2019.
[23] R.J. Good, Contact angle, wetting, and adhesion: a critical review, J. Adh. Sci. Techn. 6 (1992) 1269–1302, https://doi.org/10.1163/156856192X00629.
[24] A. Synytska, S. Michel, D. Pleul, C. Bellmann, R. Schinner, K.-.J. Eichhorn, K. Grundke, A.W. Neumann, M. Stamm, Monitoring the surface tension of reactive epoxy-amine systems under different environmental conditions, J. Adh. 80 (2004) 667–683, https://doi.org/10.1080/00218460490477639.
[25] S.A. Page, R. Mezzenga, L. Boogh, J.C. Berg, J.A. Manson, Surface energetics evolution during processing of epoxy resins, J. Colloid Interface Sci. 222 (2000) 55–62, https://doi.org/10.1006/jcis.1999.6613.][PMID: 10655125.
[26] Y. Ma, S. Nutt, Chemical treatment for recycling of amine/epoxy composites at atmospheric pressure, Polym. Degrad. Stab. 153 (2018) 307–317, https://doi.org/10.1016/j.polymdegradstab.2018.05.011.
[27] Y.-.F. Zhu, Z. Zhang, M.H. Litt, L. Zhu, High dielectric constant sulfonyl-containing dipolar glass polymers with enhanced orientational polarization, Macromol 51 (2018) 6257–6266, https://doi.org/10.1021/acs.macromol.8b00923.
[28] J.H. Kim, J.P. Rothstein, Dynamic contact angle measurements of viscoelastic fluids, J. Non-Newtonian Fluid Mech. 225 (2015) 54–61, https://doi.org/10.1016/j.jnnfm.2015.09.007.
[29] T. Kajiya, A. Daerr, T. Narita, L. Royon, F. Lequeux, L. Limat, Advancing liquid contact line on visco-elastic gel substrates: stick-slip vs. continuous motions, Soft Matter 9 (2013) 454–461, https://doi.org/10.1039/C2SM26714D.
[30] J. Nase, C. Creton, O. Ramos, L. Sonnenberg, T. Yamaguchi, A. Lindner, Measurement of the receding contact angle at the interface between a viscoelastic material and a rigid surface, Soft Matter 6 (2010) 2685, https://doi.org/10.1039/C001687J.
[31] J.H. Lee, D.W. Lee, Contact-induced molecular rearrangement of acrylic acid-incorporated pressure sensitive adhesives, Appl. Surf. Sci. 500 (2020), 144246, https://doi.org/10.1016/j.apsusc.2019.144246.
[32] A. Endruweit, G.Y.H. Choong, S. Ghose, B.A. Johnson, D.R. Younkin, N.A. Warrior, D.S.A. De Focatiis, Characterisation of tack for uni-directional prepreg tape employing a continuous application-and-peel test method, Composites Part A 114 (2018) 295–306, https://doi.org/10.1016/j.compositesa.2018.08.027.
[33] D.E. Packham, Work of adhesion: contact angles and contact mechanics, Int. J. Adh. Adh. 16 (1996) 121–128, https://doi.org/10.1016/0143-7496(95)00034-8.
[34] S. Ebnesajjad, A.H. Landrock, Adhesives Technology Handbook, 3rd ed., Elsevier Science, Amsterdam, 2015.
[35] R.J. Crossley, P.J. Schubel, N.A. Warrior, Experimental determination and control of prepreg tack for automated manufacture, Plast., Rubber Compos 40 (2011) 363–368, https://doi.org/10.1179/174328910X12777566997810.
[36] A.S.T.M. D8336-21, Standard Test Method For Characterizing Tack of Prepregs Using a Continuous Application-And-Peel Procedure, ASTM International, West Conshohocken, PA, 2021.
[37] C.A. Dahlquist, Pressure-Sensitive adhesives, in: R.L. Patrick (Ed.), Treatise On Adhesion and adhesives. Volume I: Theory, Dekker Publishing, New York, 1969, pp. 219–260.
[38] E.P. Chang, Viscoelastic windows of pressure-sensitive adhesives, J. Adh. 34 (1991) 189–200, https://doi.org/10.1080/00218469108026513.
[39] M. Fuensanta, J.M. Martin-Martinez, Influence of the hard segments content on the structure, viscoelastic and adhesion properties of thermoplastic polyurethane

pressure sensitive adhesives, J. Adhes. Sci. Technol. 34 (2020) 2652–2671, https://doi.org/10.1080/01694243.2020.1780774.
[40] M.A. Droesbeke, A. Simula, J.M. Asua, F.E. Du Prez, Biosourced terpenoids for the development of sustainable acrylic pressure-sensitive adhesives via emulsion polymerization, Green Chem 22 (2020) 4561–4569, https://doi.org/10.1039/D0GC01350A.
[41] H.-.M. Wolff, K. Irsan, Dodou, Investigations on the viscoelastic performance of pressure sensitive adhesives in drug-in-adhesive type transdermal films, Pharm. Res. 31 (2014) 2186–2202, https://doi.org/10.1007/s11095-014-1318-2.][PMID: 24599801.
[42] M. Fuensanta, J.M. Martin-Martínez, Thermoplastic polyurethane pressure sensitive adhesives made with mixtures of polypropylene glycols of different molecular weights, Int. J. Adh. Adh. 88 (2019) 81–90, https://doi.org/10.1016/j.ijadhadh.2018.11.002.
[43] W. Maassen, M.A.R. Meier, N. Willenbacher, Unique adhesive properties of pressure sensitive adhesives from plant oils, Int. J.Adh. Adh. 64 (2016) 65–71, https://doi.org/10.1016/j.ijadhadh.2015.10.004.
[44] T. Orth, M. Krahl, P. Parlevliet, N. Modler, Optical thermal model for LED heating in thermoset-automated fiber placement, Adv. Manuf. Polym. Compos. Sci. 4 (2018) 72–82, https://doi.org/10.1080/20550340.2018.1507798.
[45] Y. Peykova, S. Guriyanova, O.V. Lebedeva, A. Diethert, P. Müller-Buschbaum, N. Willenbacher, The effect of surface roughness on adhesive properties of acrylate copolymers, Int. J.Adh. Adh. 30 (2010) 245–254, https://doi.org/10.1016/j.ijadhadh.2010.02.005.
[46] A. Kowalski, Z. Czech, The effects of substrate surface properties on tack performance of acrylic pressure-sensitive Adhesives (PSAs), Int. J.Adh. Adh. 60 (2015) 9–15, https://doi.org/10.1016/j.ijadhadh.2015.03.004.
[47] M. Ciavarella, A. Papangelo, A generalized johnson parameter for pull-off decay in the adhesion of rough surfaces, Phys. Mesomech. 21 (2018) 67–75, https://doi.org/10.1134/S1029959918010095.